# Reactions of small molecules on gold single crystal surfaces

**Sónia A.C. Carabineiro[1] and Bernard E. Nieuwenhuys[2]**

www.goldbulletin.org

## Abstract

**Supported heterogeneous gold catalysts (also called "real" catalysts) have been far more studied than gold single crystal surfaces. However, the surface science approach – fundamental studies of chemistry on well defined gold surfaces under controlled conditions – is extremely important, as it contributes to the understanding of the reaction mechanisms and of the nature of active centers, which allows a better knowledge of the "real" systems. This paper presents a brief overview concerning the work carried out on gold single crystal surfaces from 2004 until recently. Results on the reactions of several molecules on gold surfaces, experimental and computational (DFT) are discussed.**

[1] *Laboratory of Catalysis and Materials, Associate Laboratory LSRE/LCM, Department of Chemical Engineering, Faculty of Engineering, University of Porto, Rua Dr. Roberto Frias, s/n, 4200-465 Porto, Portugal*

[2] *Leiden Institute of Chemistry, Leiden University, Einsteinweg 55, 2333 CC Leiden, The Netherlands, and Schuit Institute of Catalysis, Eindhoven University of Technology, P.O. Box 513, 5600 MB Eindhoven, the Netherlands*

## 1 Introduction

Since supported gold catalysts (also called "real" catalysts) are thought to have more viable commercial applications, they have received comparatively much more attention than gold single crystal surfaces [1-5]. However, the study of well defined gold surfaces using the surface science approach is of extreme importance since it contributes to the understanding of the mechanisms of gold catalysis and the nature of active centers.

In 2004, a comprehensive review was published by Hans-Joachim Freund and co-workers on "surface chemistry of catalysis by gold" [6]. In this paper, the studies carried out in the field of gold single crystal surfaces were reviewed. To the best of our knowledge, no such review on gold surface science has been published ever since. The present article presents a short review on the reactions carried out on gold single crystal surfaces from 2004 until recently, namely oxidation of CO, $NH_3$, alcohols and hydrocarbons. Both experimental and theoretical results are reviewed. The reactions of more complex molecules demand a separate review and will not be presented in this paper. This paper completes the recently published review on adsorption of small molecules on gold single crystal surfaces [7]. For general reviews on gold catalysis we refer to [3, 5-6, 8].

Au(111) is often considered as a good model surface for understanding the details of heterogeneous Au-based oxidation catalysis on the molecular level [10]. Therefore, this surface has been much more studied than other surfaces, as will be seen in this paper. The most common Au surfaces, (111), (110) and (100) are depicted in Figure 1. This figure shows the structure of the non-reconstructed surfaces. In reality, these surfaces are reconstructed [7], however, since these reconstructions are lifted upon

Figure 1

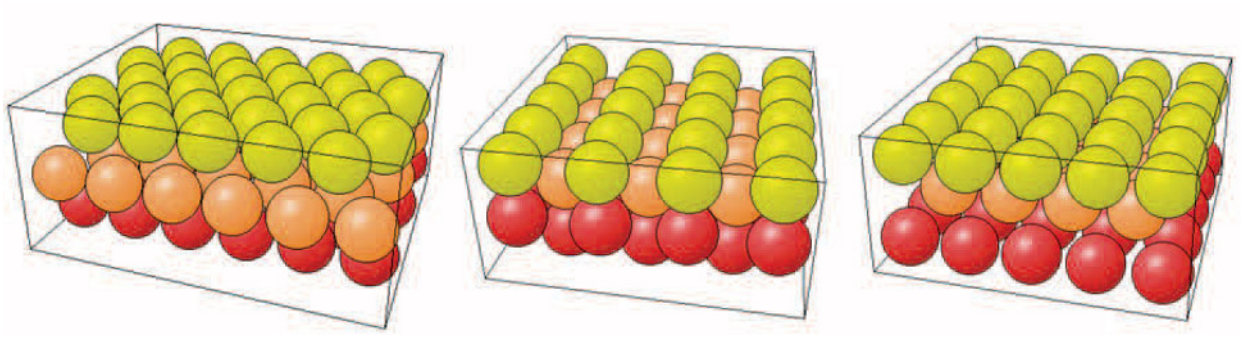

*Left to right: The structure of the non-reconstructed Au(111), Au(110) and Au(100) surfaces (adapted from the NIST Surface Structure Database [9])*

Figure 2

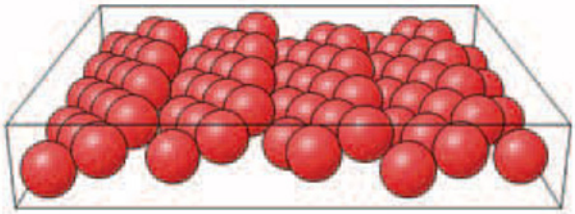

*Surface structure of the Au(321) surface (generated with Surface Explorer [11])*

adsorption, the reactions take place on the non-reconstructed surfaces.

In this context, it should be noted that in gold catalysis the gold particle size is extremely important. For many reactions, only particles smaller than ~5 nm contribute to the catalytic activity [3, 5-6, 8]. The most probable reason is that only low-coordinated surface atoms exhibit a high chemical reactivity. Hence, for a better understanding of gold catalysis, studied performed on more open surfaces such as the Au(321) surface shown in Figure 2 are very relevant.

## 2 CO oxidation

Although CO oxidation ($CO+O_2 \rightarrow CO_2$) is the most studied reaction, the mechanistic pathways are still uncertain. Recent studies have, however, provided strong evidence that CO adsorbs on the gold particles themselves [12-16], in particular on edge or step sites [14-15, 17-18]. These findings make the CO oxidation reaction on gold single crystal surfaces an interesting topic for a model study concerning CO oxidation on "real" gold catalysts.

$O_2$ dissociation has not been observed on gold surfaces and it is a very difficult process according to DFT calculations [7]. Therefore, other methods to obtain O-covered gold surfaces have been applied such as exposure to ozone, thermal dissociation of gaseous $O_2$ using hot filaments, reactive sputtering with $O_2^+$, etc [7].

Figure 3

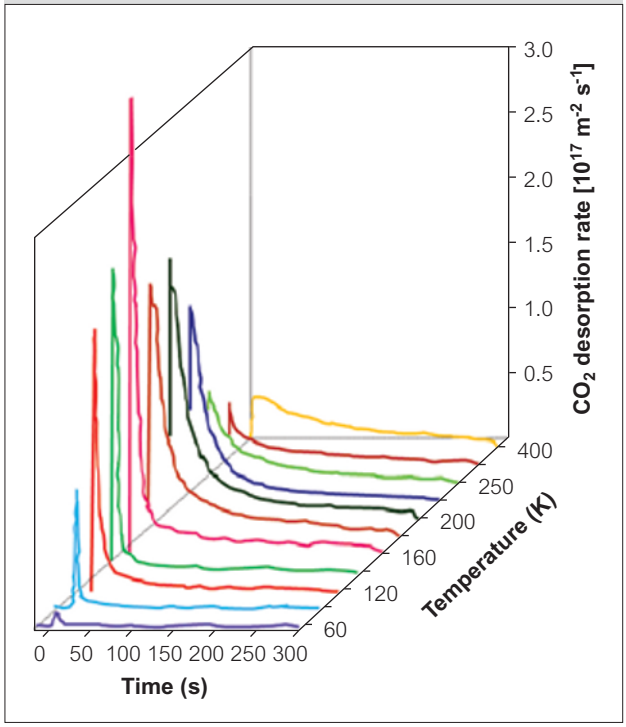


*CO oxidation over O/Au(110)-(1×2). $CO_2$ desorption rate as a function of time, between 60 and 400K (redrawn from [18])*

CO oxidation on an oxygen-precovered Au(110)-(1×2) surface [19], where oxygen atoms were prepared by electron bombardment of physisorbed $O_2$, showed an increase of the initial reaction rate between 60 and 180 K followed by a decrease up to 400 K, showing the highest initial reaction rate at a temperature of 180 K (Figure 3). At low oxygen coverages, the reaction was first-order in the oxygen coverage and had an apparent activation energy of 2 $kJmol^{-1}$. Assuming a Langmuir-Hinshelwood mechanism authors evaluated a true activation energy of 57 $kJmol^{-1}$.

For Au(111), the highest initial rate of reaction is observed at ~200 K when the surface is covered with oxygen at 200 K using ozone decomposition [20]. A similar dependence of the CO oxidation rate on reaction temperature was also reported for small gold particles oxidized using a hot filament to dissociate $O_2$. The highest rate was observed at 180 K followed by the decrease in initial rate with respect to the increase of reaction temperature [21]. The rate decrease above 200 K is unusual since the rate constant of a reaction is generally expected to increase with respect to temperature. The decrease in the rate of $CO_2$ production for reaction temperatures above 200 K is attributed to a decrease in the CO residence time with increasing temperature [19-20]. However, the distribution of oxygen on the surface may also affect the rate.

Min and Friend [22] observed CO oxidation on Au(111) populated with atomic oxygen and found out that the metastable oxygen phase is most active. Mullins et al. [23] have extended their results to reaction temperatures as low as 77 K and have also investigated the effects of oxygen coverage and annealing temperature and the role of adsorbed water. $CO_2$ can be produced efficiently from impinging a CO beam on Au(111) precovered with various O coverages (0.23-2.07 ML) at 77 K [24]. The initial adsorption probability of an impinging CO molecule was measured to be ~1/3 for an oxygen coverage of 0.45 ML at 77 K and does not vary significantly for other coverages [24]. For all oxygen coverages, prompt $CO_2$ production was observed followed by a sharp decrease due to the accumulation of CO on the surface at 77 K. Additionally, there is a strong oxygen coverage dependence at 77 K. For oxygen coverages up to 0.5 ML, $CO_2$ production increases with higher oxygen coverage due to the additional availability of oxygen. At oxygen coverages above 0.5 ML, the initial $CO_2$ production decreases with increasing oxygen coverage; likely due to the change in the nature of the adsorbed oxygen atoms and structural and electronic properties of the Au(111) surface as a function of oxygen coverage as suggested by Min and Friend [22] (and not a reduction in CO adsorption [24]). It has been shown that the adsorption of 1.0 ML of oxygen atoms on Au(111) increases the work function by 0.8 eV, indicating electron transfer from the Au substrate into the oxygen adlayer (i.e., the oxygen-induced formation of $Au^{\delta+}$ sites). The order of reactivity of atomic oxygen has been classified by these authors as: chemisorbed (metastable) oxygen > oxygen in a surface oxide (i.e., well ordered 2D Au-O phase) > oxygen in a bulk gold oxide (i.e., 3D structures containing Au and O) [22]. It appears that oxide like domains may exist only at the higher coverage, while chemisorbed oxygen on Au(111) plays a more dominate role at the lower coverages.

*Figure 4*

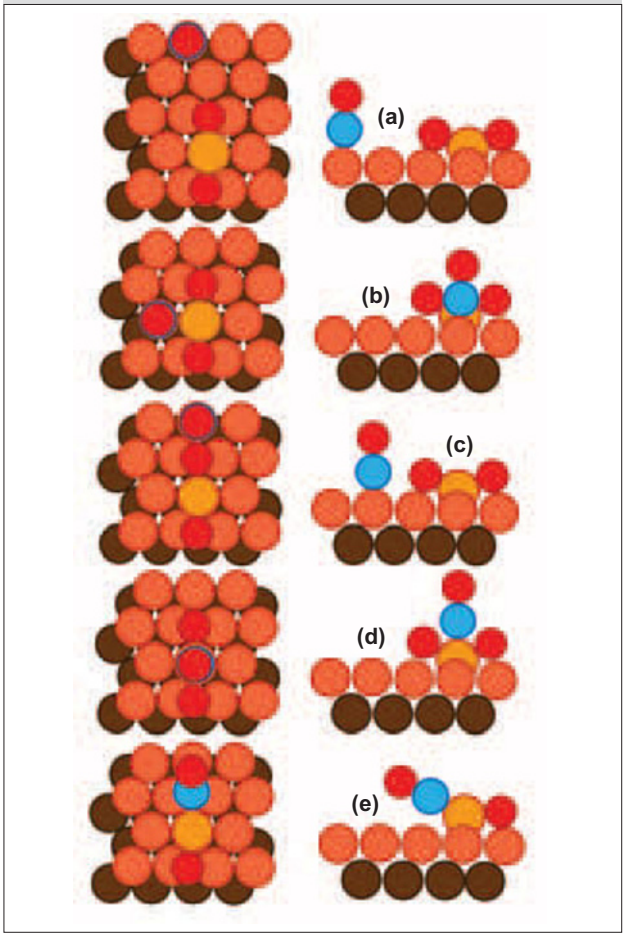


*Adsorption sites for CO on the O/Au(111) surface. Brown, orange, yellow, blue and red spheres are the first and second layers of atoms, a gold adatom lifted out of the first layer of the surface, a carbon atom, and oxygen atom, respectively (redrawn from [24])*

Recently, Friend's group also carried out DFT calculations to investigate CO oxidation on O-covered Au(111) [25]. They found out that on clean Au(111) at 500 K, CO binds transiently on top of Au atoms, spending a small fraction (~7%) of the total simulation time adsorbed on the surface. The presence of O on the surface increases the residence time for CO by more than a factor of 4 for a surface containing 0.22 ML of O (Figure 4, Table 1). On the other hand, the probability for CO adsorption decreases with oxygen coverage from 31% at 0.22 ML of oxygen to 15% at 0.55 ML of oxygen (Figure 4, Table 1). Their simulations show that the activity for CO reaction with O to yield $CO_2$ decreases with increasing oxygen coverage. This was explained by the decrease of activity to (1) the decrease in the CO adsorption probability as the oxygen coverage increases and (2) the decreasing amount of reactive chemisorbed oxygen (oxygen bound in a 3-fold site) with increasing total oxygen coverage. They showed that oxygen bound in sites of local 3-fold coordination (chemisorbed oxygen) is nearly twice more reactive than the other oxygen species observed, namely, surface and subsurface oxide.

*Table 1: Ratio of CO adsorption sites (illustrated in Figure 4) at each oxygen coverage (adapted from [24])*

| CO site | 0.22 ML | 0.33 ML | 0.55 ML |
|---|---|---|---|
| A | 0.63 | 0.24 | 0.25 |
| B | 0.17 | 0.11 | 0.16 |
| C | 0.21 | 0.47 | 0.00 |
| D | 0.00 | 0.02 | 0.52 |
| E | 0.01 | 0.16 | 0.07 |

Biener et al. [26] used ion-bombarded Au(111) surfaces as a model system to study the role of adsorbed oxygen. Their experiments show that adsorbed oxygen stabilizes low-coordination Au sites, and it is also efficiently transferred to $CO_2$ as previously observed for $SO_2$ [27]. This shows that there is a complex interplay between the activation of oxygen, the catalytic activity and the stabilization of the nanoscale structures essential for the activity.

Kim's group performed transient kinetics studies of CO oxidation on an O-precovered, stepped Au(211) single crystal surface (Figure 5) [28]. They found a behaviour similar to that observed previously on flat Au(111) and (110) surfaces; i.e., no evidence in these transient kinetics for any special reactivity associated with this stepped Au surface. The CO oxidation reaction rate was highly dependent on the initial oxygen coverage, and an apparent activation energy was determined for CO oxidation of -7.0 $kJmol^{-1}$ for $\theta_o^{init}$ = 0.9 ML.

*Figure 5*

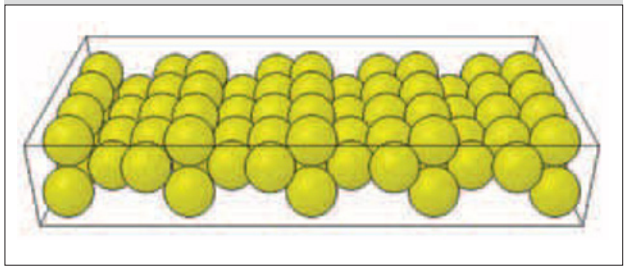

*Surface structure of the Au(221) surface (generated with Surface Explorer [11])*

The CO oxidation on the Au(321) surface (Figure 2) was investigated using DFT calculations [29]. This was done by separately studying the adsorption of isolated CO or $CO_2$ and also the coadsorption of CO+O or CO+$O_2$ on the same surface. It was found that CO adsorbs on the clean surface preferably at the kinks, and the same preference exists if atomic or molecular oxygen is coadsorbed on the Au(321) surface. $CO_2$ is only very weakly adsorbed with a large distance from the metal surface. Importantly, the formation of carbonate species or of four atoms compounds, OCOO, adsorbed on the surface is thermodynamically favourable from CO and $O_2$. The reaction of CO oxidation by atomic oxygen occurs almost without any activation energy on a reconstructed surface, whereas a moderate barrier of 58 $kJmol^{-1}$ was computed for the direct reaction with molecular oxygen occurring at the surface steps. These results suggest that the predissociation of the molecular oxygen on the Au(321) surface for the CO oxidation is energetically less favourable than the direct reaction with molecular oxygen. Finally, the products of the oxidation reaction are much more stable than the four atoms compound.

The interaction of CO/$O_2$ gas mixtures with gold has been studied by video-field ion microscopy (FIM) under truly in situ conditions on the surfaces of small Au tips by de Bocarmé et al. [30]. To elucidate the local surface composition while imaging, atom-probe studies have been performed using field pulses in a pulsed field desorption mass spectrometry (PFDMS) set-up. The interaction of pure CO with Au field-emitter tips at 300 K results in formation of Au carbonyl on the surface, and these species appear as singly and doubly charged cations $AuCO^{n+}$ and $Au(CO)_2^{n+}$ in PFDMS spectra. The formation of these

species is promoted by the presence of the high (positive) electric field required for FIM.

### 2a Influence of water and oxygen on CO oxidation

Haruta et al. showed that the addition of water in the feed stream enhances the CO oxidation reaction over supported gold particles by as much as 2 orders of magnitude [31]. This observation motivated several investigators to study the interaction of water with gold surfaces. On Au(111), water strongly interacts with oxygen atoms to make a water-oxygen complex or hydroxyls [22-23, 32-34]. Oxygen atoms from adsorbed water exchange with adsorbed oxygen adatoms on Au(111) due to rapid diffusion of transient OH groups with subsequent reversible reactions between two nearby adsorbed hydroxyl groups to adsorbed water and oxygen. DFT calculations also show that hydroxyls are readily formed by water on oxygen precovered Au(111) due to the small calculated activation barrier of 11 kJmol$^{-1}$ [33]. A recent investigation by Quiller et al. [34] suggests that isolated stable hydroxyls may not be formed and could be more transient in character. DFT calculations indicate that in the presence of $H_2O$, the barrier for CO oxidation for a select pathway is reduced to 11 kJmol$^{-1}$ compared with 24 kJmol$^{-1}$ for CO oxidation on oxygen precovered Au(111) without $H_2O$ [33]. This reduction is attributed to a concerted hydrogen transfer from one hydroxyl to another that acts to stabilize the transition state for CO oxidation and reaction at temperatures as low as 45 K.

DFT has been used to study the effect of water on the adsorption of $O_2$, O, and CO, $O_2$ dissociation, and CO oxidation on Au(111) surface [35]. It was found that, though CO oxidation with atomic O is facile with a barrier less than 28 kJmol$^{-1}$, a considerable barrier for $O_2$ dissociation (189 kJmol$^{-1}$) and weak adsorption of reactants limit the overall reactivity. The calculations show that the presence of water stabilizes substantially the adsorption of reactants, such as $O_2$, atomic O, and CO, via formation of the H bonds and/or the interactions mediated through the substrates between the adsorbates, accordingly (Figure 6). Moreover, adsorbed water molecules stabilize the transition states and various intermediates by similar interactions.

The mechanism of water-enhanced CO oxidation on oxygen precovered Au (111) surface was also theoretically studied by Zhang et al. using DFT [36]. Authors found out that water is activated by the pre-covered oxygen atom and dissociates to $OH_{ads}$ group. Then, $OH_{ads}$ reacts with $CO_{ads}$ to form chemisorbed $HOCO_{ads}$. Finally, with the aid of water, $HOCO_{ads}$ dissociates to $CO_2$. The whole process can be described as: $½H_2O_{ads}+H_2O_{ads}+½O_{ads}+CO_{ads} \rightarrow H_3O_{ads}+CO_2(g)$. Since one $CO_2$ molecule is formed with only one half of a precovered oxygen atom, that explains why more $CO_2$ is observed when water is present on oxygen pre-covered Au(111) surface. The activation energy of each elementary step is low enough to allow the reaction to proceed at low temperature.

The dynamic interaction of pure gold nanocrystals (in the form of "tips") with $H_2O$/CO gas mixtures was studied using FIM by de Bocarmé et al. [37]. While imaging with nano-scale resolution selected areas of the equivalent of ~200 atomic Au sites were analysed for their chemical composition. At room temperature the exposure of a clean Au sample to water gas at $10^{-4}$ Pa, in the presence of an electric field of ~10 V/nm,

*Figure 6*

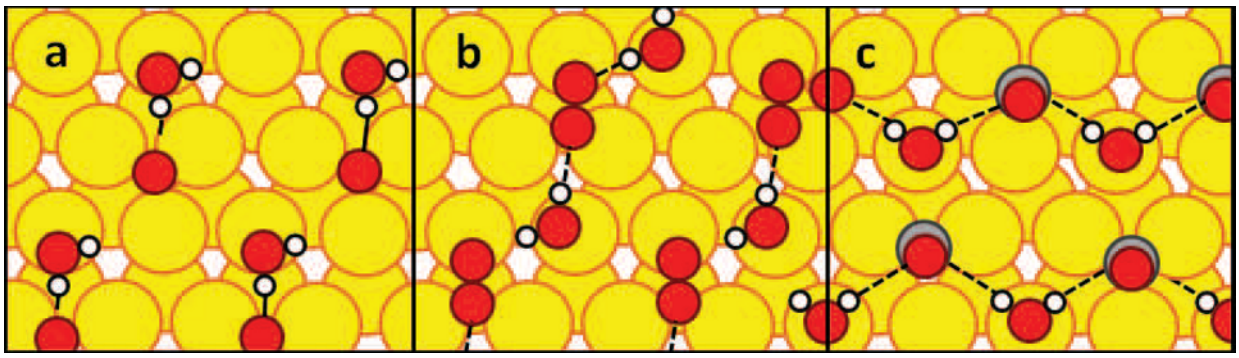


*Co-adsorbed $H_2O$ and O (a), $H_2O$ and $O_2$ (b), and $H_2O$ and CO (c) on Au(111). The metal, O, C and H atoms are represented by the yellow, red, gray and white balls, respectively (redrawn from [34])*

*Figure 7*

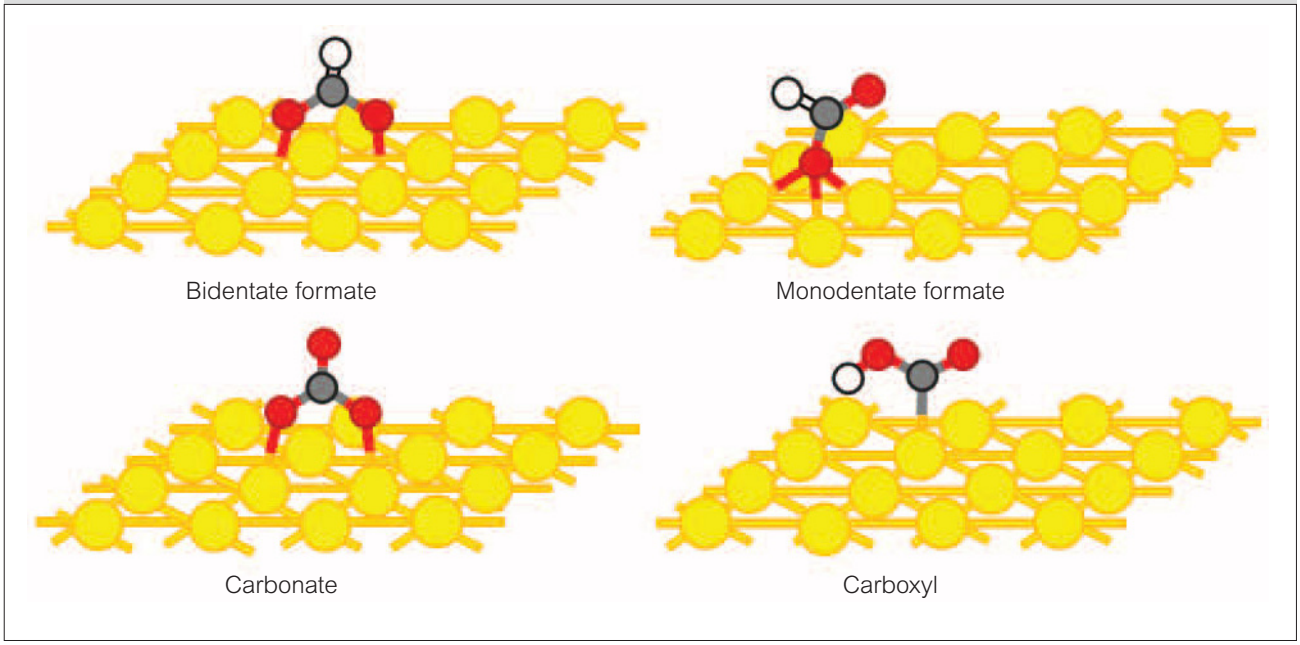


*Bonding geometries obtained by DFT calculations for bidentate formate (HCOO, $\eta^2$-O.O=, monodentate formate (HCOO, $\eta_1$-O), carbonate ($CO_3$, $\eta^2$-O,O), and a carboxyl intermediate (HOCO, $\eta^1$-C) on Au(111) (redrawn from [39])*

led to water adsorption and formation of bright patterns in FIM. Additional exposure to CO gas at $5\times10^{-3}$ Pa led to the removal of the water layer. Surface hydroxyl was also detected mass spectrometrically and the respective ion intensities decreased during the titration with CO. The results suggest that gold nanocrystals, in the absence of an oxidic support, may be active in the reaction between water and CO at temperatures as low as 300 K in the presence of an electric field of ~10 V/nm.

### 2b Role of carbonate, formate and carboxyl species in CO oxidation

The carbonate formation and decomposition ($CO_3 \rightarrow CO_2+O_{ads}$) reaction on gold is important from the point of view of low temperature CO oxidation. Carbonate formation has been proposed as a possible reaction intermediate in CO oxidation in several papers.

Mullins and co-workers studied carbonate formation on Au(111) [38-39]. Experimental results supported by DFT calculations show carbonate formation and reaction on atomic oxygen precovered Au(111) [39]. Oxygen mixing was observed when $^{16}O_{ads}$ precovered Au(111) was exposed to isotopically labelled $CO_2$ ($C^{18}O_2$) at surface temperatures ranging from 77-400 K and initial oxygen coverages ranging from 0.18-2.1 ML. Subsequent desorption of isotopically mixed oxygen ($^{16}O^{18}O$, mass 34) was observed as a byproduct of carbonate formation and decomposition on the surface. Authors also reported the enhanced formation and decomposition of carbonate from the reaction of $C^{18}O_2$ preadsorbed on Au(111) with an $^{16}O$ atomic beam [38]. The amount of formed carbonate increases significantly (by a factor of ~4) compared to thermally accommodated $C^{18}O_2$ and $^{16}O_{ads}$ coadsorbed on the Au(111) surface. The results suggest that the reaction occurs prior to the accommodation of the incident atomic oxygen via a precursor-mediated mechanism [38].

The role of formate (HCOO), carbonate ($CO_3$) and carboxyl (HOCO) species as possible intermediates in the water-gas shift reaction (WGS): $OH_{ads}$ + $CO_{(g)} \rightarrow CO_{2(g)}$ + $0.5H_{2(g)}$ reaction on Au(111) were also studied [40]. Adsorbed HCOO, $CO_3$, and OH species were prepared by adsorbing formic acid, carbon dioxide, and water on a Au(111) surface precovered with 0.2 ML of atomic oxygen. It was found that HCOOH interacts only weakly with Au(111), but on O/Au(111) it dissociates its acidic H to yield adsorbed formate. Results of NEXAFS, IR, and density-functional calculations indicate that the formate adopts a bidentate ($\eta^2$-O,O) configuration on Au(111) (Figure 7). According to DFT calculations, the bidentate configuration for HCOO is more stable than a monodentate ($\eta$-O) configuration by

~62 kJmol$^{-1}$. Since the HCOO groups are stable on Au(111) up to temperatures near 350 K, it is not likely that formate is a key intermediate for the WGS reaction at low temperatures. In fact, the formation of this species could lead eventually to surface poisoning. Compared to formate species, carbonate species formed by the reaction of $CO_2$ with O/Au(111) has low stability, decomposing at temperatures between 100 and 125 K, and should not poison the gold surface. The results of DFT calculations predict a bidentate ($\eta^2$-O,O) configuration for carbonate on Au(111) (Figure 7). Neither HCOO nor $CO_3$ was detected during the reaction of CO with OH on Au(111) at 90-120 K. It was suggested that the reaction of CO with OH on Au(111) proceeds with HOCO as a possible intermediate [40].

## 3 $SO_2$ formation and oxidation

Friend's group studied the reaction of sulfur and oxygen with the Au(111) surface [26, 41]. They found by STM that the herringbone reconstruction of Au(111) lifts when either S or O is deposited on the surface. They attributed the structural change to the reduction of tensile surface stress via charge redistribution by these electronegative adsorbates. This lifting of the reconstruction was accompanied by the release of gold atoms from the structure. At high coverage, clusters of gold sulfides or gold oxides form by abstraction of gold atoms from regular terrace sites of the surface. Concomitant with the restructuring is the release of gold atoms from the herringbone structure to produce a higher density of low-coordinated Au sites by forming serrated step edges or small gold islands. These undercoordinated Au atoms may play an essential role in the enhancement of catalytic activity of gold in reactions such as oxygen dissociation or $SO_2$ decomposition [41].

Biener et al. also studied the interaction of $SO_2$ with oxygen-sputtered Au(111) ($\theta_{oxygen} \leq 0.35$ ML) by monitoring the oxygen and sulfur coverages as a function of $SO_2$ exposure (Figure 8) [26]. Two reaction regimes were observed: oxygen depletion followed by sulfur deposition. An enhanced, transient sulfur deposition rate is observed at the oxygen depletion point. This effect is specifically pronounced if the Au surface is continuously exposed to $SO_2$. The enhanced reactivity towards S deposition seems to be linked to the presence of highly reactive, undercoordinated Au atoms. Adsorbed oxygen appears to stabilize, but also to block these sites. In absence of the stabilization effect of adsorbed oxygen, i.e., at the oxygen depletion point, the enhanced reactivity decays on a timescale of a few minutes.

*Figure 8*

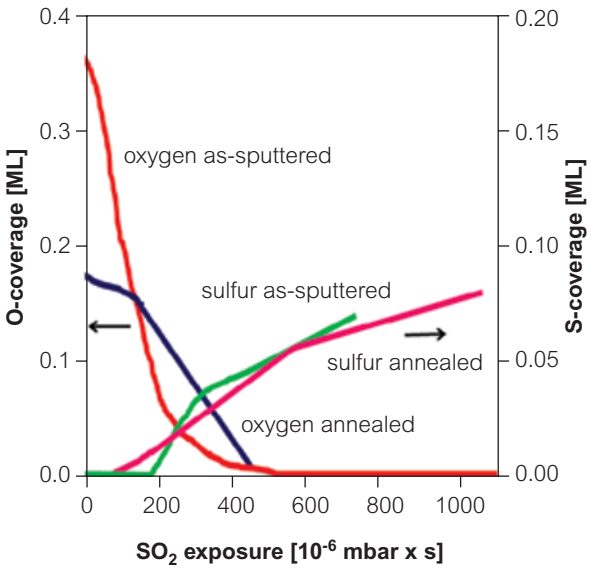


*AES data showing oxygen and sulfur coverages obtained from the oxygen-sputtered Au(111) surface (500 eV/~1 μA/10 min/300K) as a function of $SO_2$ exposure at 300K. The oxygen coverage decreases with increasing $SO_2$ exposure and sulfur deposition is only observed after depletion of oxygen. Annealing of an oxygen-sputtered surface at 400K before $SO_2$ exposure at 300K reduces the initial coverage by ~40%, but does not change the behaviour with respect to oxygen depletion and sulfur deposition (redrawn from [25])*

## 4 Alkene oxidation and epoxidation

The partial oxidation of hydrocarbons is one of the most important chemical transformations in petroleum-based industrial processes, as the oxygenated products are used as key intermediates in organic synthesis [5]. Scheme 1 shows the structures of several unsaturated hydrocarbons often used in oxidation reactions.

*Scheme 1*

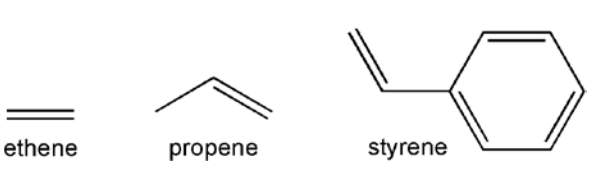


*Schematic structures of ethene, propene and styrene*

### 4a Ethene oxidation and epoxidation

Although Au(100) does not adsorb oxygen at either 295 K or 80 K, Carley et al. [42] found out that a Ba modified Au(100) surface is active in oxygen dissociation resulting, through surface diffusion of oxygen adatoms, in the formation of a chemisorbed oxygen adlayer. This oxygen species is inactive for ethene oxidation, as is the oxygen species pre-adsorbed at an Au(100)-Ba surface at 80 K, and the clean Au(100)-Ba surface. However, when molecularly adsorbed ethene present at a Au(100)-Ba surface at 80 K is exposed to dioxygen and warmed to 140 K, surface carbonate is observed. Authors concluded that a transient oxygen species is the oxidant.

Torres and Illas [43] performed a DFT study of the epoxidation mechanism of ethene on Au(111). They found that, once atomic oxygen is adsorbed on the surface, partial oxidation to ethene oxide becomes possible. Calculated transition state theory rate constants for the elementary steps involved in the reaction predict a selectivity of Au(111) toward epoxide of 40%, in good agreement with the recent experimental findings for styrene epoxidation on Au(111) [44], described in 4c (as styrene is often employed as a model molecule for ethene in UHV model studies).

### 4b Propene oxidation and epoxidation

Epoxidation of propene does not occur to any significant extent on oxygen-covered Au(111) [21, 45]. However, acrolein is clearly produced by oxygen covered Au(111). Metastable, disordered oxygen on Au is more active and more selective for propene oxidation, since the metastable phase is favoured at low temperature [21].

DFT calculations showed that the Au(111) surface is inefficient for the selective oxidation of propene even when it is precovered by atomic oxygen [46]. Results show that the necessary formation of oxametallacycle reaction intermediates (OMME) (Figure 9) on Au is thermodynamically favoured but kinetically inhibited. It was suggested that the failure of extended gold surfaces to epoxidize higher alkenes arises from the high sensitivity of the molecular mechanism toward changes in the basic character of adsorbed oxygen.

*Figure 9*

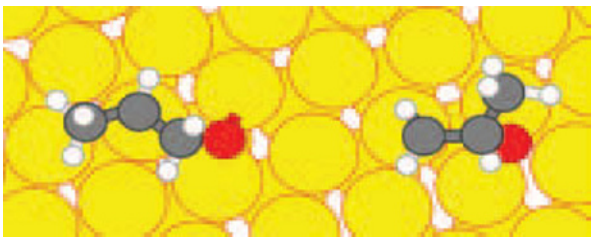

*OMME intermediates (OMME1 (left) and OMME2 (right) involved in propene oxidation on Au(111) (redrawn from [45])*

However, the metastable oxygen phase on oxidized Au(111) showed to be active for partial oxidation of propene, based on temperature-programmed reaction using atomic oxygen on Au(111) [21, 45]. Specifically, atomic oxygen (0.3 ML) was prepared on Au(111) by exposure to ozone at 200 K followed by exposure to propene at 130 K. Although partial oxidation of propene is promoted by oxidized Au(111), the epoxide which is formed on supported Au nanocatalysts is not observed. It is possible that this difference might be due to an effect of the metal oxide support in the nanocatalysts. The products of partial oxidation of propene are acrolein, carbon suboxide, and acrylic acid.

The reaction product distribution obtained by Min and Friend is significantly different from previous studies of propene oxidation on Au(111) and Au(110), in which the reaction yielded major combustion products and a small amount of partial oxidation products, possibly acrolein [47]. This difference may be due to different oxygen bonding resulting from the different method and surface temperature: atomic oxygen was created by passing $O_2$ over a glowing tungsten filament at 300 K.

### 4c Styrene oxidation and epoxidation

Deng and Friend reported on the selective oxidation of styrene by O-covered Au(111) [44]. Oxygen atoms were deposited on Au by electron bombardment of condensed $NO_2$. The gold surface changes its structure and releases Au atoms from the surface; however, the surface maintains a smooth morphology [48]. Oxygen deposited using this method is relatively strongly bound to the Au(111) surface, desorbing as $O_2$ at ~550 K [49]. The oxidation of styrene on chemisorbed oxygen covered Au(111) selectively yields styrene oxide, benzoic acid, and benzeneacetic acid (Scheme 2). Most styrene is selectively oxidized with only ~20% completely combusting. Authors showed that extended Au surfaces are capable of promoting selective hydrocarbon oxidation once the oxygen atoms are seeded on the surface. Thus, the seemingly unique oxidation activity of supported Au nanoparticles might be due to an ability of these supported nanoparticles to dissociate $O_2$ or to a specific role of the oxidic support.

The influence of subsurface oxygen and surface roughness on the selectivity and activity for styrene oxidation was also investigated on Au(111) by Friend's group [50]. Buried oxygen and a rough surface morphology was created by $O_2^+$ sputtering of Au(111). The effect of surface roughness was specifically investigated by creating a similarly rough surface morphology using $Ar^+$ sputtering and subsequently oxidizing with ozone. The major products of styrene oxidation were styrene epoxide, benzoic acid, $CO_2$ and water. Subsurface oxygen does not significantly affect either the product distribution or the overall amount of styrene conversion. Surface roughness leads to an increase of the overall amount of styrene that is oxidized and reduces the selectivity for, styrene epoxidation.

Xue et al. studied the reaction mechanism for the elective oxidation of styrene on an oxygen preadsorbed Au(111) surface by DFT calculations [51]. The results demonstrate that the pendant phenyl group in the styrene structure is nearly parallel to the surface and the center of the phenyl is on the three-fold-hollow site. The results of the calculations showed that the reaction mechanism consists of two steps: first, the OMME intermediate is formed and then the products. It was found that the energy profile for such reaction is very similar to that reported for selective oxidation of ethene on oxygen-adsorbed Au(111), and the rate-controlling step is the same (i.e., from OMME to final product). More importantly, the presented DFT calculations suggest that the mechanism via the OMME (2) (i.e., the preadsorbed atomic oxygen bound to the $CH_2$ group involved in $C_6H_5$–CH=$CH_2$) to produce styrene epoxide is kinetically favoured than that of OMME(1) (Scheme 2).

Friend and co-workers showed that chlorine coadsorbed with oxygen on Au(111) significantly enhances the selectivity of styrene epoxidation by inhibiting secondary oxidation, especially complete combustion, formation of organic acids, and the deposition of residual carbon [52]. The temperature required for formation of styrene oxide is also lowered relative to O-covered Au(111), indicating faster kinetics for epoxidation.

Gao et al. [53] studied styrene epoxidation on $Au_{38}$ and $Au_{55}$ clusters, using DFT calculations. Results

*Scheme 2*

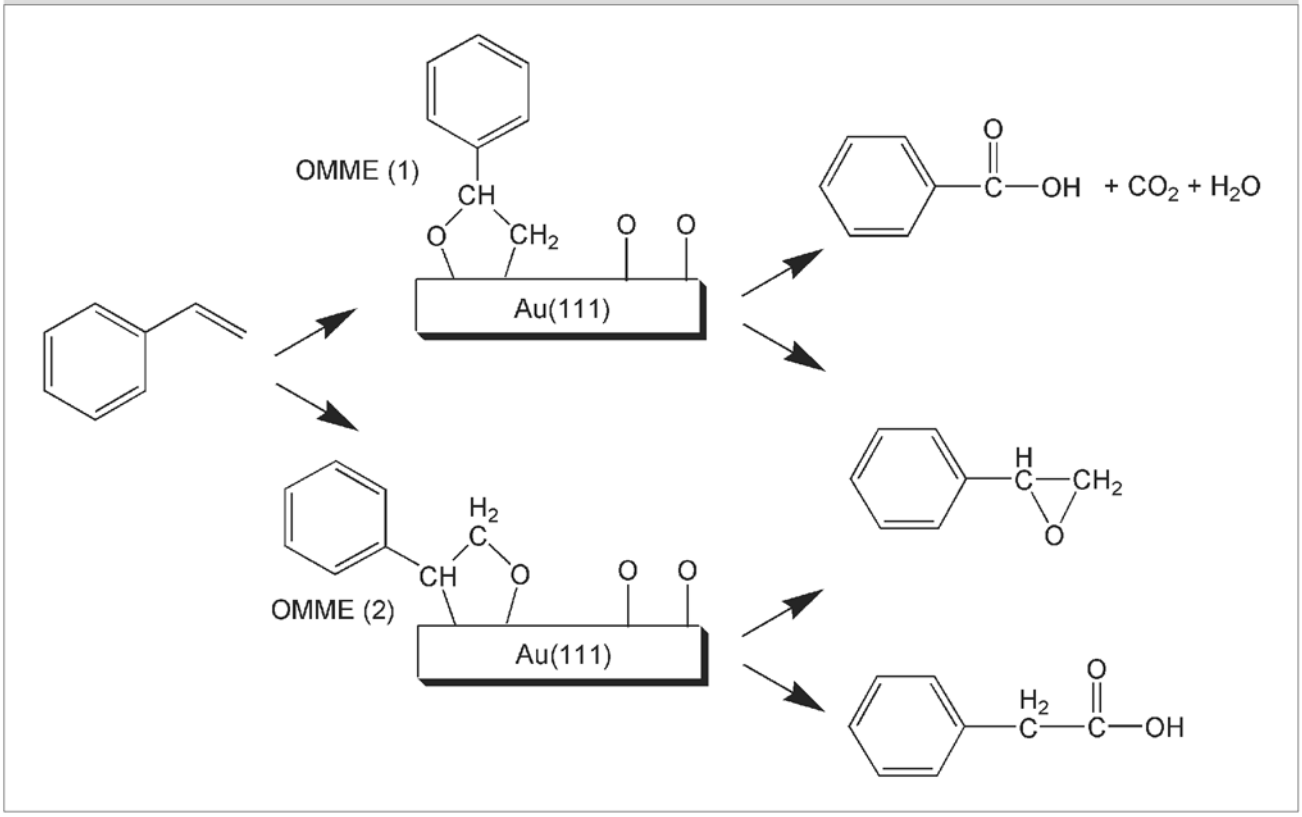


*Proposed reaction for styrene oxidation on O-Au(111) surface (adapted from [43, 50])*

suggest that epoxidation proceeds via a surface oxametallacycle intermediate. Two parallel reaction pathways coexist on the $Au_{38}$ cluster: $O_2$ dissociates before epoxidation and $O_2$ directly reacts with styrene, whereas only the latter pathway is found on the $Au_{55}$ cluster, which is induced by different geometries of the $Au_{38}$ and $Au_{55}$ clusters. The mechanism of $O_2$ directly reacting is essentially determined by the electronic resonance between electronic states of adsorbed intermediates and Au atoms at reaction sites. Moreover, Au atoms correlated with the reaction on the $Au_{38}$ cluster are more electropositive than those on the $Au_{55}$ cluster, which leads to a higher catalytic activity of the former. Thus, the $Au_{38}$ cluster should be the size threshold for epoxidation catalysis, being consistent with the obtained barrier values.

**4d N-addition to styrene**

Friend's group reported also on functionalization of an olefin with NH on Au(111), which may have advantages and mechanistic differences when compared to aziridination in solution or in other methods of activating ammonia for amination [10, 54]. Aziridines are structurally analogous to epoxides and may be formed by addition of a nitrene group to the olefin. Functionalization of styrene to form N-containing hydrocarbons, e.g. 2-phenylaziridine, benzonitrile, and benzyl nitrile, is achieved by reaction with adsorbed $NH_{ads}$ and $N_{ads}$ on Au(111) (Scheme 3) [10, 54]. Electron-induced decomposition of condensed $NH_3$ was used to produce $NH_{ads}$, $N_{ads}$ and $H_{ads}$ on Au(111) at 110 K. The addition of NH to styrene results in the production of 2-phenylaziridine, whereas adsorbed N and H atoms lead to the formation of nitriles benzonitrile and benzyl nitrile and, respectively, ethylbenzene. Nitrene addition to styrene was thus promoted by a gold surface, which indicates that such reactions should also be possible with heterogeneous Au catalysts.

## 5 Selective oxidation of ammonia

Selective catalytic oxidation of ammonia to nitrogen and water is potentially an ideal technology for removing ammonia from $NH_x$-containing waste gases [22, 55-56]. In addition, from a scientific point of view, the oxidation of ammonia is interesting because three N-containing products can be formed, viz. $N_2$, $N_2O$ and NO. The selectivity of this reaction to $N_2$ or to NO on Au(111) is tunable by the amount of surface-bound oxygen. $N_2$ recombination is hindered by a barrier of 91 $kJmol^{-1}$ whereas that of NO formation is 99 $kJmol^{-1}$ [55-56]. For Au(111) with low oxygen coverages, ammonia can be selectively oxidized to form water and $N_2$ without any trace of nitrogen oxides [22]. Abstraction of hydrogen from ammonia via the high basic character of O atoms is the initial step in the surface decomposition of $NH_3$ and the formed hydroxyl is also a stripping agent for $NH_x$ dehydrogenation as seen in Scheme 4 [56]. Atomic oxygen or hydroxyl-assisted dehydrogenation steps have lower barriers than recombination reactions.

*Scheme 3*

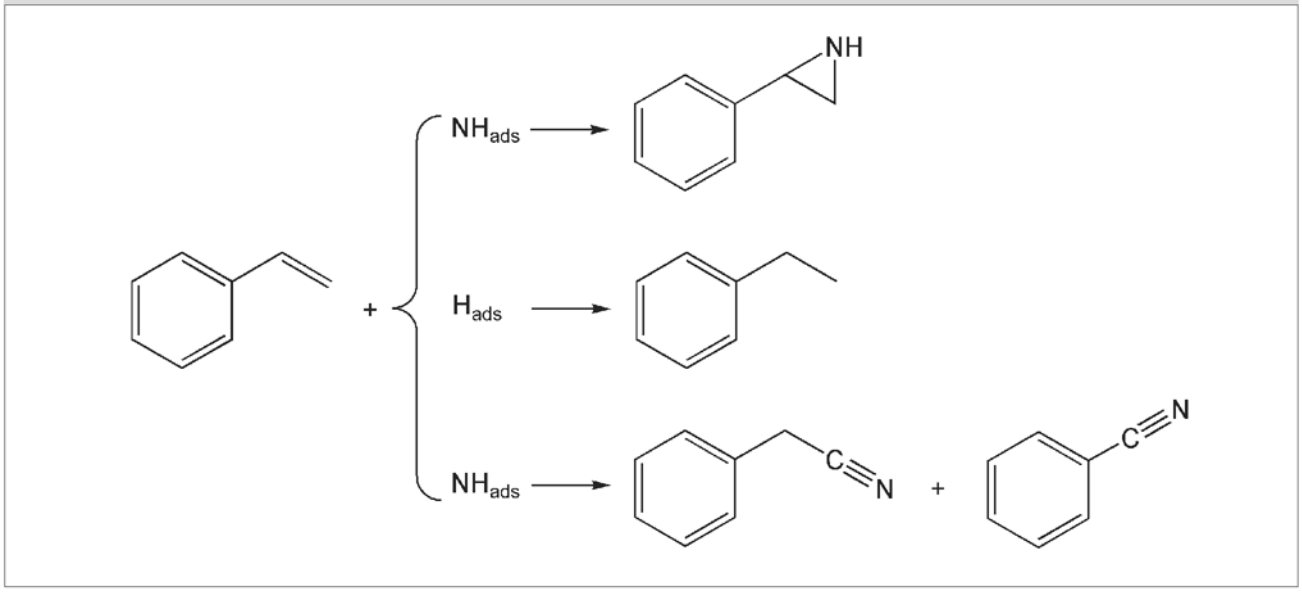


*Styrene reaction on $NH_x$-covered Au(111) surface (adapted from [53])*

*Scheme 4*

**Activation steps:**

$NH_3 \leftrightarrow NH_2 + H$
$NH_3 + O \leftrightarrow NH_2 + OH$
$NH_3 + OH \leftrightarrow NH_2 + H_2O$

**Dehydrogenation steps:**

$NH_2 \leftrightarrow NH + H$
$NH_2 + O \leftrightarrow NH + OH$
$NH_2 + OH \leftrightarrow NH + H_2O$
$NH \leftrightarrow N + H$
$NH + O \leftrightarrow N + OH$
$NH + OH \leftrightarrow N + H_2O$

**Termination steps:**

$N + N \leftrightarrow N_2$
$N + O \leftrightarrow NO$

*Dehydrogenation reactions of ammonia on the clean, oxygen and hydroxyl covered Au(111) surface (according to ref. [55])*

## 6 Oxidation of amines

As derivatives of ammonia, amines have been investigated extensively due to their importance in many heterogeneously catalyzed processes. Propylamine (n-$C_3H_7NH_2$), for example, can be selectively oxidized to the associated nitrile and aldehyde dependent on oxygen coverage on Au(111) (Scheme 5) [57]. At low oxygen coverage (i.e., $\theta_O$ < 0.5 ML) propylamine initially undergoes N-H bond breaking to produce propionitrile and water, while the formation of propionitrile, propaldehyde, water, CO, $CO_2$, and $N_2O$ was observed at higher oxygen coverages [22, 57].

## 7 Oxidation of NO

Nitrogen oxides exhibit interesting chemistry on bulk gold surfaces (see ref. [7]). From a practical point of view, both the selective catalytic reduction of $NO_x$, and the selective oxidation of NO is interesting [22]. Compared to the oxidation of CO, the oxidation of NO, $2NO+O_2 \rightarrow 2NO_2$, has not been studied in detail over gold-based catalysis.

It has been shown by experimental data and also by DFT calculations that the NO uptake on the Au(111) surface is enhanced by the presence of oxygen adatoms [58-60]. At temperatures above 200 K, $NO_2$ production becomes limited by the surface lifetime of the adsorbed NO species. Below 200 K, nitric oxide can react with surface oxygen to form a chemisorbed $NO_2$ product. Based on an analysis involving a kinetic competition between desorption of the NO molecule and reaction with O adatoms, an activation energy of 20 $kJmol^{-1}$ is estimated for the 0.95 ML O/Au(111) surface [58].

Torres et al. also used the DFT approach to study the reaction of NO with atomic O on the Au(111)

*Scheme 5*

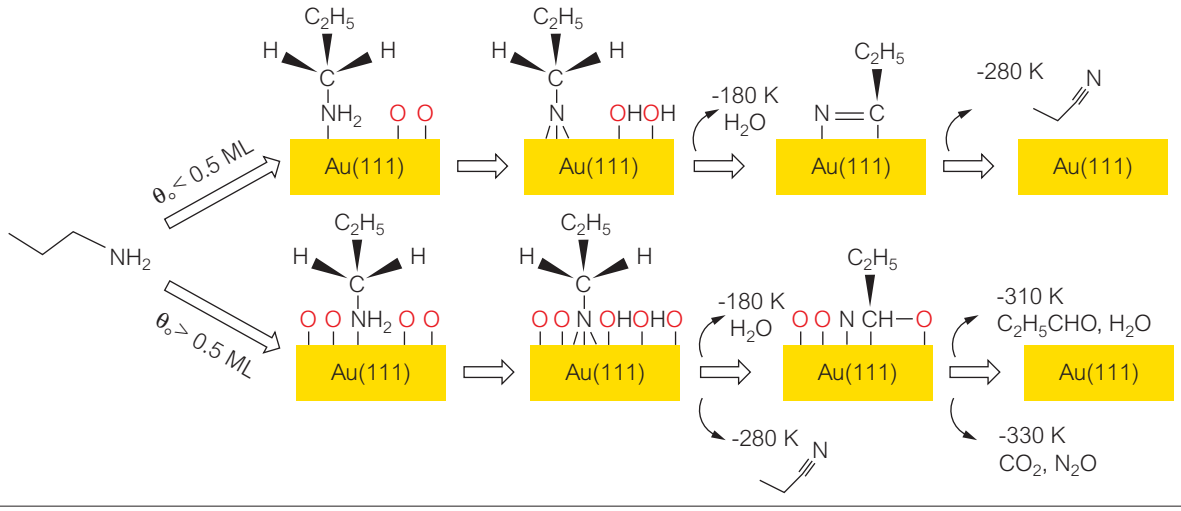


*Proposed mechanism of propylamine oxidation on O/Au(111) surface (redrawn from [56])*

surface at low temperature to form $NO_2$ [60]. The very small adsorption energy found for NO on regular Au(111) surface, ~20 kJmol$^{-1}$, implies that the NO adsorption detected on Au(111) at ~175 K takes place on defects. (NO+O)/Au(111) species form $NO_2$/Au(111) without an activation barrier, releasing 170 kJmol$^{-1}$ [60].

NO dissociation with and without the presence of hydrogen on the Au(321) surface (Figure 10) was investigated using DFT calculations [61]. The role of hydrogen in the reaction of NO dissociation is studied by comparing four different routes (i.e., direct dissociation of NO on the clean surface and paths involving reaction with hydrogen adatoms prior to N-O bond cleavage). In the latter situation, two routes via a NOH intermediate were considered, producing N*+OH* or N*+$H_2O$*, and another route via a NHOH intermediate was also considered, yielding NH* and OH* species. The calculations predict that the kinetically most favourable route is that producing nitrogen adatoms and water, i.e., NO*+2H*→ N*+$H_2O$* via the NOH* intermediate. This reaction is exothermic (106 kJmol$^{-1}$) and the energy barriers for the separate NO*+H*→NOH* and NOH*+H*→ N*+$H_2O$* reactions are equal to 48 kJmol$^{-1}$. A similar energy barrier was calculated for the reaction of the dissociation of molecular hydrogen on the stepped surface studied here, which is one-half of the barrier calculated in the case of the planar Au(111) surface. The thermodynamically more favourable reaction is that via the NHOH intermediate (144 kJmol$^{-1}$). The kinetically least favourable path for NO dissociation on Au(321) is that occurring on the clean surface with an energy barrier of 336 kJmol$^{-1}$; this reaction is also highly endothermic (> 211 kJmol$^{-1}$). The presented results suggest that the presence of hydrogen is a necessary condition for NO dissociation on this stepped surface.

*Figure 10*

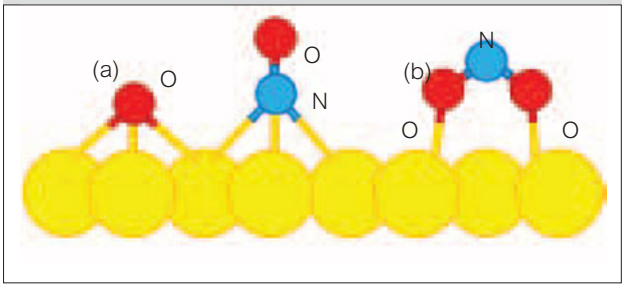


*Calculated a) initial state - NO+O/Au(111), and b) final state - $NO_2$/Au(111), complexes of the oxidation reaction of adsorbed NO by co-adsorbed oxygen on Au(321) surface. Au large yellow atoms, O – small red, N- small blue. (redrawn from [60])*

## 8 Alcohol oxidation

The selective oxidation of alcohols into aldehydes or ketones is an important process in the synthesis of fine chemicals [5].

### 8a Methanol oxidation

Oxidation of $CH_3OH$ has been investigated on Au(111) [62-63]. An adsorbed methoxy [$CH_3O_{ads}$] intermediate is formed on oxygen precovered Au(111) [22, 62-63]. At low oxygen coverages the methoxy further reacts to methyl formate when the surface with atomic oxygen (via ozone decomposition) was exposed to methanol at 200 and 160 K, respectively [63]. However, for the surface with coadsorbed atomic oxygen (via *O-plasma*) and methanol at 77 K, methoxy only decomposes to produce $H_2O$, CO, and $CO_2$, while no other partial oxidation products or derivatives such as formaldehyde, formic acid, or methyl formate were detected [62-63]. This difference indicates that the preparation method of atomic oxygen and the surface temperature in which reactants were adsorbed play a crucial role in determining the reaction pathway.

### 8b Ethanol oxidation

In contrast to methanol, ethanol is selectively oxidized on O-Au(111), as indicated by the formation of acetaldehyde (and water) for low oxygen coverages [22]. No other partial oxidation products, such as methane, ethane, ethene, ethanol, acetic acid, ethene oxide, methyl formate, and ethyl acetate, as well as C1-containing species (e.g., CO, $CO_2$, formaldehyde, and formic acid) were detected during the reaction [64]. Ethanol initially undergoes O-H bond cleavage (producing ethoxide) followed by selective β-C-H bond (R to the oxygen) elimination to form acetaldehyde and water on atomic oxygen precovered Au(111). Isotopic experiments provide evidence of the absence of cleavage of the C-O and the γ-C-H bonds [64]. At higher oxygen coverages (i.e., 1.0 ML), in addition to acetaldehyde and water, $CO_2$ was also formed during the reaction due to the cleavage of the γ-C-H bond and the C-C bond.

Several authors showed that ethanol can be transformed into its carbonyl compounds, namely acetaldehyde, ethyl acetate, acetic acid, and ketone on Au(111) (Figure 11) with O-containing Au nanoparticles formed as a result of Au atom release upon ozone exposure [65-66]. Ethoxy and acetate are identified as two key reaction intermediates during the oxidation of ethanol. The formation of acetaldehyde is due to the deprotonation of ethoxy,

which can be further oxidized into acetate. The low-temperature formation of the ester, ethyl acetate, proceeds via the coupling of acetaldehyde with excess surface ethoxy. These reaction pathways appear relevant to heterogeneous processes catalyzed by supported gold nanoparticles, thus providing further insight into the mechanistic origin of gold-mediated oxidation of alcohols [65-66].

### 8c Propanol oxidation

Similar to the surface oxidation chemistry of ethanol, both 1-propanol and 2-propanol can be oxidized, on oxygen precovered Au(111), to propaldehyde and acetone, respectively (Scheme 6) [67]. Remarkably, the reactions are 100% selective to propaldehyde or acetone at low surface temperatures (i.e., 300-325 K) for all oxygen precoverages investigated [22]. For high oxygen precoverages (i.e., above 0.5 ML) and surface temperatures (350-400 K), a small amount of $CO_2$ (less than 5%) was formed.

## 9 Concluding remarks

This review shows that the surface chemistry on gold surfaces is very rich. Most of the reactions on single crystal surfaces has been studied on Au(111). This surface is considered a good model for understanding the details of gold catalysis at the molecular level.

However, since the adsorption of molecules and atoms is very sensitive to the structure of the gold surface (see ref. 7) there is an urgent need to study the same reactions on open gold surfaces with low-coordinated gold atoms. The few available

Figure 11

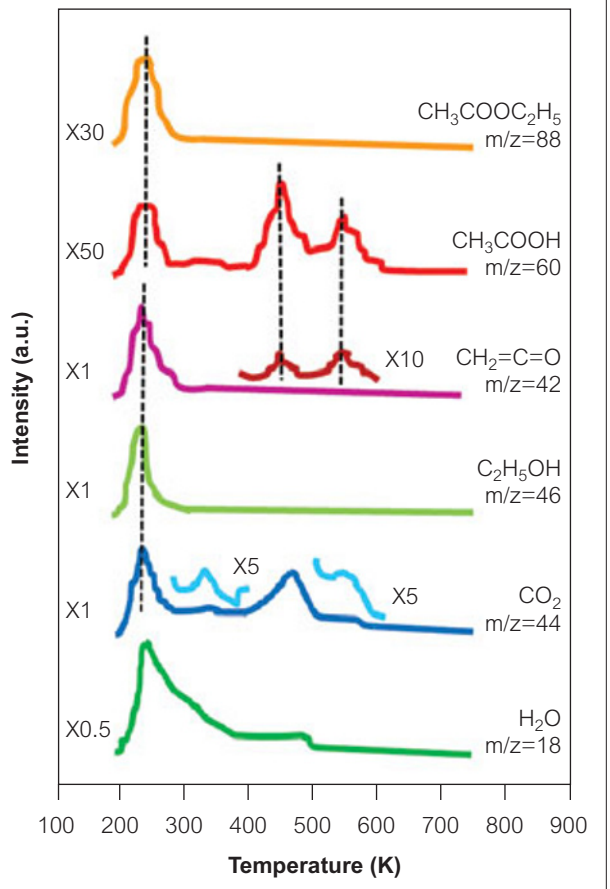


*TPR spectra of the oxidation of ethanol on the Au(111) surface. The surface is precovered with oxygen adatoms with a coverage of 0.4 ML. The dotted lines denote the fragment peaks that align with their corresponding parent ion peaks (redrawn from [64])*

Scheme 6

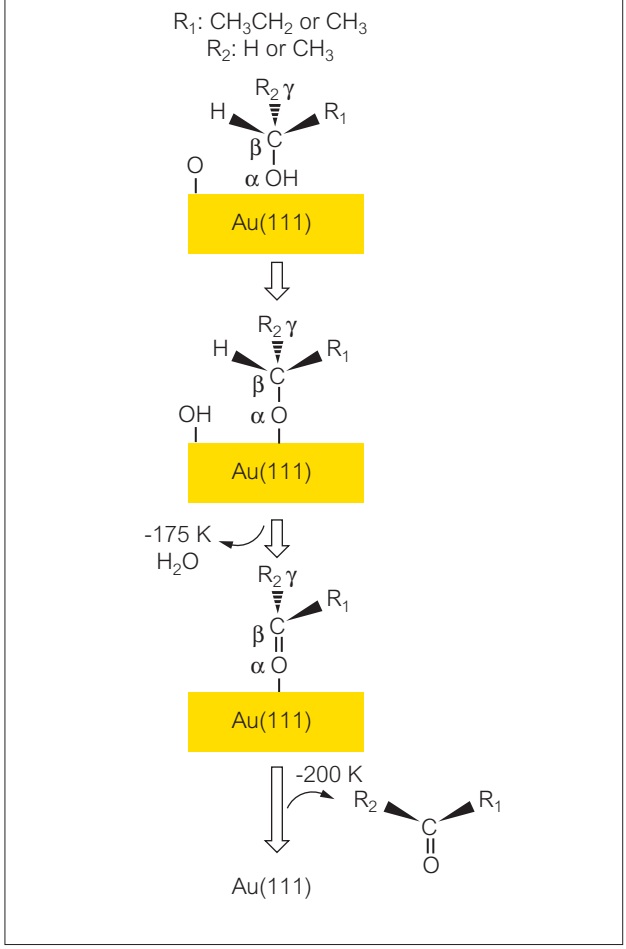


*Proposed reaction for selective oxidation of 1-propanol or 2-propanol to propaldehyde or acetone on O-Au(111) surface (redrawn from [66])*

data presented in this review show indeed that the chemistry on these gold surfaces is very different than on the Au(111) surface.

In addition, we would like to add that a "real" (supported) gold catalyst consists of gold nanoparticles on a support. For high activity, an "active" support, usually a transition metal oxide or ceria, is used or it is added to the less active alumina support. These "active" oxides ($MO_x$) may work as a co-catalyst or promoter [5, 70].

In oxidation reactions one of the crucial steps is the activation of oxygen. As we have discussed before, $O_2$ dissociation has not been observed on gold surfaces and it is a very difficult process according to DFT calculations [7]. It has been shown that the "active" oxygen can be supplied by the $MO_x$ [71]. Therefore, for a real understanding of oxidation reactions on gold catalysts, fundamental studies using model catalysts containing both gold and $MO_x$ are needed. The $MO_x$ may also play an important role in the formation of carbonates, formates and carboxyl species in CO oxidation (see Section 2c). We hope to write a review on the subject (adsorption and reactions on model catalysts consisting of gold surfaces/nanoparticles and $MO_x$) in the near future.

## Acknowledgements

SACC is grateful to Fundação para a Ciência e Tecnologia, Portugal, for financing (CIENCIA 2007 program).

## About the authors

**Sónia A.C. Carabineiro** obtained her Ph.D. in Catalysis at the New University of Lisbon, Portugal under the supervision of Isabel F. Fonseca. She was a post doc in Leiden University, The Netherlands, working with Bernard E. Nieuwenhuys. She returned to Portugal and after another post doc position at the Technical University of Lisbon, where she worked with Pedro T. Gomes, she moved to the University of Porto as an assistant researcher in the group of José L. Figueiredo. Sónia is currently working in the field of gold catalysed oxidation reactions.

**Bernard E. Nieuwenhuys** received his Ph.D. in Chemistry from the Leiden University, the Netherlands, under the tutelage of W.M.H. Sachtler. Between 1975 and 1976 he was a postdoctoral fellow at the University of California, Berkeley, where he worked under the supervision of G.A. Somorjai. In 1977 he joined the Faculty of Chemistry at the Leiden University. He is a professor in heterogeneous catalysis and surface chemistry, also part-time at the Eindhoven University of Technology, the Netherlands.

## References

1 C.W. Corti and R.J. Holliday, *Gold Bull.*, 2004, **37**, 20
2 C.W. Corti, R.J. Holliday and D.T. Thompson, *Appl. Catal. A*, 2005, **291**, 253
3 G.C. Bond, C. Louis and D.T. Thompson, *Catalysis by Gold*. Catalytic Science Series, ed. G.J. Hutchings. Vol. 6. 2006, London, United Kingdom: Imperial College Press
4 C.W. Corti, R.J. Holliday and D.T. Thompson, *Top. Catal.*, 2007, **44**, 331
5 S.A.C. Carabineiro and D.T. Thompson, *Catalytic Applications for Gold Nanotechnology*, in *Nanocatalysis*, E.U. Heiz and U. Landman, Editors. 2007, Springer-Verlag: Berlin, Heidelberg, New York. p. 377
6 R. Meyer, C. Lemire, S.K. Shaikhutdinov and H. Freund, *Gold Bull.*, 2004, **37**, 72
7 S.A.C. Carabineiro and B.E. Nieuwenhuys, *Gold Bull.*, 2009, **42**, 288
8 S.A.C. Carabineiro and D.T. Thompson, *Gold Catalysis*, in *Gold: Science and applications*, C. Corti and R. Holliday, Editors. 2010, CRC Press, Taylor and Francis Group, Boca Raton, London, New York, pp.89
9 Available from: http://www.fhi-berlin.mpg.de/~hermann/Balsac/SSDpictures.html#A
10 X.Y. Deng, T.A. Baker and C.M. Friend, *Angew. Chem., Int. Ed.*, 2006, **45**, 7075
11 Available from: http://w3.rz-berlin.mpg.de/~rammer/surfexp_prod/SXinput.html
12 M.A.P. Dekkers, M.J. Lippits and B.E. Nieuwenhuys, *Catal. Lett.*, 1998, **56**, 195
13 M.A.P. Dekkers, M.J. Lippits and B.E. Nieuwenhuys, *Catal. Today*, 1999, **54**, 381
14 M. Haruta, *Cattech*, 2002, **6**, 102
15 A. Haruta, *Chem. Rec.*, 2003, **3**, 75
16 D.H. Wang, Z.P. Hao, D.Y. Cheng, X.C. Shi and C. Hu, *J. Mol. Catal. A: Chem.*, 2003, **200**, 229
17 H.H. Kung, M.C. Kung and C.K. Costello, *J. Catal.*, 2003, **216**, 425
18 T.V.W. Janssens, B.S. Clausen, B. Hvolbaek, H. Falsig, C.H. Christensen, T. Bligaard, J.K. Nørskov, *Top. Catal.*, 2007, **44**, 15

19 J.M. Gottfried and K. Christmann, *Surf. Sci*., 2004, **566-568**, 1112
20 B.K. Min, A.R. Alemozafar, D. Pinnaduwage, X. Deng and C.M. Friend, *J. Phys. Chem. B*, 2006, **110**, 19833
21 J. Kim, Z. Dohnalek and B.D. Kay, *J. Am. Chem. Soc*., 2005, **127**, 14592
22 B.K. Min and C.M. Friend, *Chem. Rev*., 2007, **107**, 2709
23 J.L. Gong and C.B. Mullins, *Acc. Chem. Res*., 2009, **42**, 1063
24 J.L. Gong, R.A. Ojifinni, T.S. Kim, J.D. Stiehl, S.M. Mcclure, J.M. White and C.B. Mullins, *Top. Catal*., 2007, **44**, 57
25 T.A. Baker, C.M. Friend and E. Kaxiras, *J. Chem. Theory Comput*., 2010, **6**, 279
26 J. Biener, M.M. Biener, T. Nowitzki, A.V. Hamza, C.M. Friend, V. Zielasek and M. Baumer, *ChemPhysChem*, 2006, **7**, 1906
27 M.M. Biener, J. Biener and C.M. Friend, *Surf. Sci*., 2005, **590**, L259
28 E. Samano, J. Kim and B.E. Koel, *Catal. Lett*., 2009, **128**, 263
29 J.L.C. Fajin, M. Cordeiro and J.R.B. Gomes, *J. Phys. Chem. C*, 2008, **112**, 17291
30 T.V. De Bocarmé, T.D. Chau and N. Kruse, *Surf. Interface Anal*., 2007, **39**, 166
31 M. Date, M. Okumura, S. Tsubota and M. Haruta, *Angew. Chem., Int. Ed*., 2004, **43**, 2129
32 T.S. Kim, J. Gong, R.A. Ojifinni, J.M. White and C.B. Mullins, *J. Am. Chem. Soc*., 2006, **128**, 6282
33 R.A. Ojifinni, N.S. Froemming, J. Gong, M. Pan, T.S. Kim, J.M. White, G. Henkelman and C.B. Mullins, *J. Am. Chem. Soc*., 2008, **130**, 6801
34 R.G. Quiller, T.A. Baker, X. Deng, M.E. Colling, B.K. Min and C.M. Friend, *J. Chem. Phys*., 2008, **129**, 064702
35 H.Y. Su, M.M. Yang, X.H. Bao and W.X. Li, *J. Phys. Chem. C*, 2008, **112**, 17303
36 W.H. Zhang, Z.Y. Li, Y. Luo and J.L. Yang, *Chin. Sci. Bull*., 2009, **54**, 1973
37 T.V. De Bocarmé, T.D. Chau and N. Kruse, *Surf. Sci*., 2006, **600**, 4205
38 J.L. Gong and C.B. Mullins, *J. Phys. Chem. C*, 2008, **112**, 17631
39 R.A. Ojifinni, J. Gong, N.S. Froemming, D.W. Flaherty, M. Pan, G. Henkelman and C.B. Mullins, *J. Am. Chem. Soc*., 2008, **130**, 11250
40 S.D. Senanayake, D. Stacchiola, P. Liu, C.B. Mullins, J. Hrbek and J.A. Rodriguez, *J. Phys. Chem. C*, 2009, **113**, 19536
41 B.K. Min, A.R. Alemozafar, M.M. Biener, J. Biener and C.M. Friend, *Top. Catal*., 2005, **36**, 77
42 A.F. Carley, P.R. Davies, M.W. Roberts and A.M. Shah, *Catal. Lett*., 2005, **101**, 137
43 D. Torres and F. Illas, *J. Phys. Chem. B*, 2006, **110**, 13310
44 X.Y. Deng and C.M. Friend, *J. Am. Chem. Soc*., 2005, **127**, 17178
45 X.Y. Deng, B.K. Min, X.Y. Liu and C.M. Friend, *J. Phys. Chem. B*, 2006, **110**, 15982
46 A. Roldan, D. Torres, J.M. Ricart and F. Illas, *Journal of Molecular Catalysis a-Chemical*, 2009, **306**, 6
47 K.A. Davis and D.W. Goodman, *J. Phys. Chem. B*, 2000, **104**, 8557
48 B.K. Min, X. Deng, D. Pinnaduwage, R. Schalek and C.M. Friend, *Physical Review B*, 2005, **72**, 121410
49 X. Deng, B.K. Min, A. Guloy and C.M. Friend, *J. Am. Chem. Soc*., 2005, **127**, 9267
50 V. Zielasek, B.J. Xu, X.Y. Liu, M. Baumer and C.M. Friend, *J. Phys. Chem. C*, 2009, **113**, 8924
51 L.Q. Xue, X.Y. Pang and G.C. Wang, *J. Comput. Chem*., 2009, **30**, 438
52 D.S. Pinnaduwage, L. Zhou, W.W. Gao and C.M. Friend, *J. Am. Chem. Soc*., 2007, **129**, 1872
53 W. Gao, X.F. Chen, J.C. Li and Q. Jiang, *J. Phys. Chem. C*, 2010, **114**, 1148
54 X. Deng and C.M. Friend, *Surf. Sci*., 2008, **602**, 1066
55 J.L. Gong, R.A. Ojifinni, T.S. Kim, J.M. White and C.B. Mullins, *J. Am. Chem. Soc*., 2006, **128**, 9012
56 N. Lopez, M. Garcia-Mota and J. Gomez-Diaz, *J. Phys. Chem. C*, 2008, **112**, 247
57 J.L. Gong, T. Yan and C.B. Mullins, *Chem. Commun*., 2009, 761
58 S.M. McClure, T.S. Kim, J.D. Stiehl, P.L. Tanaka and C.B. Mullins, *J. Phys. Chem. B*, 2004, **108**, 17952
59 W.H. Zhang, Z.Y. Li, Y. Luo and J.L. Yang, *J. Chem. Phys*., 2008, **129**, 134708
60 D. Torres, S. González, K.M. Neyman and F. Illas, *Chem. Phys. Lett*., 2006, **422**, 412
61 J.L.C. Fajin, M. Cordeiro and J.R.B. Gomes, *J. Phys. Chem. C*, 2009, **113**, 8864
62 J. Gong, D.W. Flaherty, R.A. Ojifinni, J.M. White and C.B. Mullins, *J. Phys. Chem. C*, 2008, **112**, 5501
63 B.J. Xu, X.Y. Liu, J. Haubrich, R.J. Madix and *C.M.* Friend, *Angew. Chem., Int. Ed*., 2009, **48**, 4206
64 J.L. Gong and C.B. Mullins, *J. Am. Chem. Soc*., 2008, **130**, 16458
65 R.J. Madix, C.M. Friend and X.Y. Liu, *J. Catal*., 2008, **258**, 410
66 X.Y. Liu, B.J. Xu, J. Haubrich, R.J. Madix and C.M. Friend, *J. Am. Chem. Soc*., 2009, **131**, 5757
67 J.L. Gong, D.W. Flaherty, T. Yan and C.B. Mullins, *ChemPhysChem*, 2008, **9**, 2461
68 I. Nakamura, A. Takahashi and T. Fujitani, *Catal. Lett*., 2009, **129**, 400
69 J. Kim, E. Samano and B.E. Koel, *Surf. Sci*., 2006, **600**, 4622
70 B.E. Nieuwenhuys, A.C. Gluhoi, E.D.L. Rienks, C.J. Weststrate, C.P. Vinod, *Catal. Today*, 2005, **100**, 49
71 A.C. Gluhoi, H.S. Vreeburg, J.W. Bakker, B.E. Nieuwenhuys, *Appl. Catal. A*, 2005, **291**, 145